src64 and tec29 are required for microfilament contraction during Drosophila cellularization

Jeffrey H. Thomas and Eric Wieschaus*

Howard Hughes Medical Institute, Molecular Biology Department, Washington Road, Princeton University, Princeton, NJ 08544, USA
*Author for correspondence (e-mail: ewieschaus@princeton.edu)

Summary

Formation of the *Drosophila* cellular blastoderm involves both membrane invagination and cytoskeletal regulation. Mutations in *src64* and *tec29* reveal a novel role for these genes in controlling contraction of the actin-myosin microfilament ring during this process. Although membrane invagination still proceeds in mutant embryos, its depth is not uniform, and basal closure of the cells does not occur during late cellularization. Double-mutant analysis between *scraps*, a mutation in anillin that eliminates microfilament rings, and *bottleneck* suggests that microfilaments can still contract even though they are not organized into rings. However, the failure of rings to contract in the *src64 bottleneck* double mutant suggests that *src64* is required for microfilament ring contraction even in the absence of Bottleneck protein. Our results suggest that *src64*-dependent microfilament ring contraction is resisted by Bottleneck to create tension and coordinate membrane invagination during early cellularization. The absence of Bottleneck during late cellularization allows *src64*-dependent microfilament ring constriction to drive basal closure.

Key words: *Drosophila*, Cellularization, Blastoderm formation, Src64, Tec29, Scraps, Anillin, Bottleneck, Microfilament, Contractile

Introduction

The mechanisms that establish the cellular blastoderm of the early *Drosophila* embryo are as yet incompletely understood. During cellularization, the peripheral syncytial nuclei of the wild-type embryo are surrounded by membrane to form an epithelial blastoderm. This is accomplished by the simultaneous and uniform invagination of membrane between the peripheral nuclei (Mazumdar and Mazumdar, 2002; Schejter and Wieschaus, 1993a). At the leading edge of membrane invagination, known as the cellularization front, are stable infoldings of plasma membrane known as furrow canals (Lecuit and Wieschaus, 2000; Fullilove and Jacobson, 1971). The base of each furrow canal is rich in the cytoskeletal proteins F-actin and myosin II, and may provide a contractile force that helps pull membrane inward (Schejter and Wieschaus, 1993a; Young et al., 1991; Warn and Robert-Nicoud, 1990). To identify additional cytoskeleton components involved in early embryogenesis, we used deficiencies to screen part of the third chromosome (J.H.T. and E.W., unpublished). Analysis of the genes that mapped to a region identified in this screen revealed a cellularization phenotype associated with deletions in a *Drosophila src* homolog, *src64* (*Src64B* – FlyBase).

Src proteins have been shown to be involved in the regulation of the cytoskeleton and its components during the reorganization of microfilaments in both lamellipodia and filopodia in fibroblasts (Frame et al., 2002; Thomas and Brugge, 1997; Thomas et al., 1995). The structure of members of the Src family of consists of an N-terminal myristoylation site, an SH3 domain, an SH2 domain, a tyrosine kinase domain and a C-terminal regulatory domain. The myristoylation of Src protein allows it to be tethered to the plasma membrane, whereas the SH3 and SH2 domains serve to bind proline-rich recognition sequences and phosphotyrosine residues, respectively (Harrison, 2003; Frame, 2002; Thomas and Brugge, 1997). In vertebrates, Src has been shown to activate Tec family non-receptor tyrosine kinases, which are similar to Src in that they have an SH3, an SH2 and a kinase domain, and are also thought to interact with gene products associated with the cytoskeleton (Smith et al., 2001; Thomas and Brugge, 1997).

In *Drosophila*, there are two *src* homologs, *src42* (*Src42A* – FlyBase) and *src64*, and one Tec family kinase encoded by *tec29* (*Btk29A* – FlyBase) (Takahashi et al., 1996; Katzen et al., 1990; Vincent et al., 1989; Gregory et al., 1987; Wadsworth et al., 1985; Simon et al., 1985; Simon et al., 1983). There is evidence that these genes play a role in cytoskeletal regulation. During embryogenesis, for example, *tec29 src42* double mutants and *src42; src64* double mutants have dorsal closure defects associated with reduced quantities of phosphotyrosine and filamentous actin (Tateno et al., 2000). However, the best-studied example of *src64* and *tec29* involvement in cytoskeletal regulation is found in the formation and growth of the ring canals during oogenesis. The ring canals are formed by the sequential addition of several different proteins, including Src64 and Tec29, to an actin- and anillin-rich arrested cleavage furrow left from the incomplete divisions of the female germ cells (Sokol and Cooley, 1999; Dodson et al., 1998; Guarnieri et al., 1998; Roulier et al., 1998; Robinson and Cooley, 1996; Majajan-Miklos and Cooley, 1994; Robinson et al., 1994).

After assembly and the loss of anillin localization, the ring canal enters a growth phase (Robinson and Cooley, 1996). In *src64* and *tec29* mutants, ring canal growth is stunted so that fully grown ring canals are never formed (Dodson et al., 1998; Guarnieri et al., 1998; Roulier et al., 1998). The ultimate consequence of Src activity may be the phosphorylation of Kelch, an actin bundling protein that regulates actin polymerization by reversible cross-linking (Kelso et al., 2002; Tilney et al., 1996).

Here we report that *src64* and *tec29* play a role in the cytoskeletal dynamics that occur during cellularization of the *Drosophila* embryo. *src64* and *tec29* are essential for the contraction of the microfilament rings that are present in the cellularization front, and appear to play a role in membrane invagination and in subsequent basal closure. This role is distinct from that of *scraps* (anillin), which is required for the formation of these rings but is not directly required for their contraction. Using double-mutant analysis, we show that a previously identified regulator of cellularization, *bottleneck* (*bnk*), acts by countering the *src64*-dependent contraction of the microfilament rings, but shows only an additive effect in combination with *scraps*. Finally, we propose a mechanical model for cellularization, taking into account the similar and different roles played by microfilament contraction and *src64*-independent forces.

Materials and methods

Fly strains and genetics

OreR was used as the wild-type strain. Unless otherwise noted, other strains are described by Lindsley and Zimm (Lindsley and Zimm, 1992) or The Flybase Consortium (The Flybase Consortium, 2003). *src64ᴰ17* was used as the *src64* mutation in these experiments; it is a strong reduction-of-function allele that eliminates most of the Src64 protein (Dodson et al., 1998). *Df(3L)10H* and *Df(3L)Flex14* (Nose et al., 1994) were used as the deficiencies for *src64*. *tec29ᵏ00206* was used as the *tec29* allele as it eliminates the *tec29* transcript, as assayed by in situ hybridization (Roulier et al., 1998). Baba et al. (Baba et al., 1999) and Sinka et al. (Sinka et al., 2002) report some *tec29* activity in this mutant suggesting that it is a strong reduction-of-function allele. Other alleles used include *scrapsᴿˢ* and *scrapsᴾQ* (Schüpbach and Wieschaus, 1989), and *Df(3R)tll-e* to delete *bnk* (Schejter and Wieschaus, 1993b).

tec29 germline clones were constructed essentially as previously described (Roulier et al., 1998; Guarnieri et al., 1998). OreR males were crossed into *tec29* germline clone females to generate embryos.

Histology and image analysis

To visualize myosin, Even-skipped, Armadillo, Anillin and Bottleneck proteins, embryos were methanol heat-fixed (Wieschaus and Nusslein-Volhard, 1998) and stained with rabbit anti-myosin (a gift from C. Field, Harvard Medical School, Boston, MA), guinea pig anti-Eve, mouse anti-Arm (N27A1), rabbit anti-anillin (a gift from C. Field, Harvard Medical School, Boston, MA) or rat anti-Bottleneck (5) (Schejter and Wieschaus, 1993b) antibody, respectively. To visualize Tec29 protein and phosphotyrosine-containing proteins, embryos were fixed in a formaldehyde/phosphate buffer in the presence of heptane (Oda et al., 1994) and stained with either mouse anti-Tec29 (I19) antibody (Roulier et al., 1998; Vincent et al., 1989) or mouse anti-phosphotyrosine (PY20) antibody (Transduction Laboratories, BD Biosciences). Src64 protein was visualized by fixing embryos as described for Tec29 protein, or by using 4% paraformaldehyde in lieu of formaldehyde and staining with rabbit anti-Src64 antibody (a gift from T. Xu, Yale University, New Haven,

CT). Primary antibodies were detected with Alexa 488- and Alexa 546-conjugated goat antisera (Molecular Probes). Nuclei were visualized by staining with Hoechst dye. Sagittal sections were obtained optically. Cross-sections were made by using a 26-gauge hypodermic needle to manually cut fixed and stained embryos. Embryos were mounted in Aquapolymount (Polysciences), and were observed using a Nikon E800 fluorescence microscope and a Zeiss LSM-510 confocal microscope.

Image analyses were performed using ImageJ software for Macintosh (W. Rasband, NIH; http://rsb.info.nih.gov/ij/). Circularity was calculated by Image J software as the normalized ratio of area to perimeter ($c=4\pi A/p^2$, where c=circularity, A=area and p=perimeter) so that in a true circle this ratio is one. The mean circularity is reported as the circularity index. Samples were analyzed by calculating the circularities of approximately 25 contiguous basal openings of embryos of the same age and the results were compared using a *t*-test assuming unequal sample variances. Subsamples of 20 contiguous basal openings were also compared using a Wilcoxon-Mann-Whitney test. Genotypes were considered different only if both tests produced *P* values of less than 0.001.

To analyze cellularization dynamics, six wild-type and six *src64* embryos were mounted on biofoil membrane (Kendro) in halocarbon oil 27 (Sigma), covered with a coverslip supported by another coverslip on either side of the embryo and examined under bright field illumination using a Nikon E800 microscope. Time-lapse images were collected every 60 seconds using a CoolSNAP cf camera (Photometrics) and IPLab 3.6.3 image processing software for Macintosh (Scanalytics). Cellularization front depth was measured using ImageJ software.

Results

Src64 mediates cytoskeletal contraction at the cellularization front

Mutations in *src64* that eliminate Src64 protein expression during oogenesis cause defects in the ring canals formed in the nurse cell-oocyte complex. Despite these structural defects, a significant fraction of homozygous mutant females produce eggs that are fertilized and give rise to viable embryos (Dodson et al., 1998). In addition to the reduced egg production, reduced hatch rate and increased incidence of short embryos observed by Dodson et al. (Dodson et al., 1998), we observed that syncytial blastoderm stage *src64* embryos also display a weak nuclear fallout phenotype, such that some nuclei have dropped out of the periphery before cellularization. This phenotype is much weaker than that found in mutants such as *nuf*, *SCAR* and *Arpc1* (Rothwell et al., 1998; Zallen et al., 2002). We examined older embryos of *src64ᴰ17* homozygous females for the level of Src64 expression and its intracellular localization during cellularization. In wild-type embryos, Src64 protein localizes most intensely to the cellularization front at the beginning of cycle 14, in a domain that roughly overlaps that of other cytoskeletal proteins such as anillin and myosin. Embryos from *src64ᴰ17* homozygous females stained for Src64 protein show no specific staining of the cellularization front and essentially lack all non-background staining (Fig. 1A,B).

In wild-type embryos, the cellularization front marks the site of membrane invagination between adjacent nuclei of the syncytial blastoderm. Actin and myosin at the base of each furrow canal may provide a contractile force that helps pull invaginating membrane inward (Schejter and Wieschaus, 1993a). In cross-sections of early cellularization stage wild-type embryos, each furrow canal has a rounded appearance and
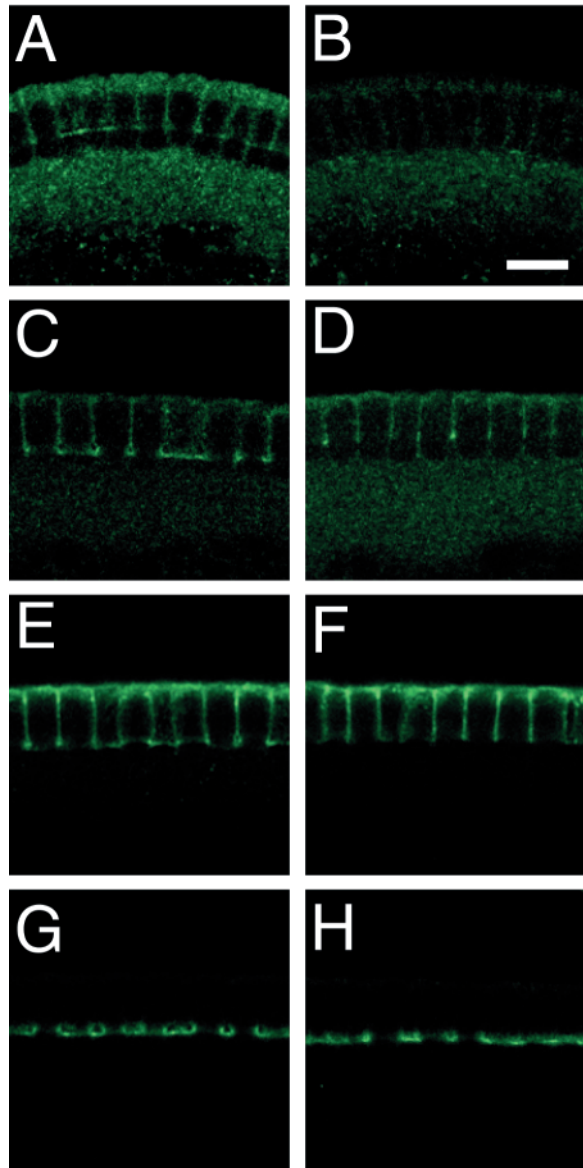
Fig. 1. Src64, Tec29 and anillin localization in wild-type and *src64* mutants during cellularization. Cross-sections of a wild-type (A) and a *src64*$^{\Delta 17}$ mutant (B) embryo, and sagittal sections of wild-type (C,E,G) and *src64*$^{\Delta 17}$ mutant (D,F,H) embryos during cellularization. Embryos were stained with antibodies to Src64 (A,B), Tec29 (C,D), phosphotyrosine (E,F) and anillin (G,H). (A) Src64 protein localizes predominantly to the cellularization front in wild-type embryos but is absent in *src64*$^{\Delta 17}$ mutant embryos (B). (C,D) Tec29 localizes strongly to the cellularization front and less strongly to the apico-lateral membrane in both wild-type and *src64* embryos. (E,F) Phosphotyrosine-containing proteins localize to the cellularization front in both wild-type embryos and *src64* embryos. (G,H) Anillin localizes to the cellularization front in both wild-type and *src64* embryos. Scale bar: 10 μm.

Table 1. Microfilament ring circularity index values

Genotype	Early cellularization	Late cellularization
Wild type	0.93	0.94
src64	0.80	0.81
tec29	ND	0.82
scra	0.89	0.73
bnk	0.92	0.91
scra; bnk	ND	0.90
src64 bnk	ND	0.85

ND, the circularity index value was not determined because the circularity of the microfilament rings did not differ between early and late cellularization.

adjacent furrow canals are at a similar depth, giving the cellularization front a uniform and taut appearance around the circumference of the embryo (Fig. 2A). In *src64*$^{\Delta 17}$ mutant embryos, the furrow canals are less rounded, and adjacent furrow canals extend to different depths in the embryo, giving the cellularization front a wavy, slack appearance as if it were no longer under tension (Fig. 2B). Viewed from the surface, the early cellularization front in wild-type embryos appears as a network of tightly apposed, densely staining myosin microfilament rings surrounding the nuclei (Fig. 2C). In *src64*$^{\Delta 17}$ embryos, the microfilament rings are not rounded but instead are irregular in shape and sometimes sharply angular (Fig. 2D). We have used the ImageJ circularity assay to estimate the tension of the microfilament ring, based on the assumption that rings under tension will more closely resemble a circle and will therefore have a circularity index close to 1.0 (W. Rasband, NIH; see Materials and methods). During early cellularization, the microfilament rings of the wild-type embryo have a circularity of 0.93 (Table 1). At the same stage in *src64*$^{\Delta 17}$ embryos, the microfilament rings enclose roughly the same area as those of wild type, but have a longer perimeter such that the circularity ratio is 0.80 (Table 1), a significant deviation from that of wild type (*P*<0.001). The longer perimeter is the result of the microfilament ring having a convoluted and meandering shape, such that indentations occur in the rings. The deviation from circularity suggests that the microfilament rings are not under tension and are held together in a loose mesh.

As the cellularization front passes the bases of the peripheral nuclei, the actin-myosin cytoskeleton undergoes a reorganization such that the microfilament rings are no longer linked. Each microfilament ring now contracts in diameter so as to lead to the gradual basal closure of the cells into a narrow stalk (Schejter and Wieschaus, 1993b). This contraction causes the lumen of the furrow canals in wild-type embryos to expand into a flask-like shape (Fig. 2E). The microfilament rings are round and constricted (Fig. 2G), and have a circularity of 0.94 (Table 1). In *src64*$^{\Delta 17}$ embryos the furrow canals do not expand (Fig. 2F). The microfilament rings are large, less rounded and convoluted (Fig. 2H), they enclose a greater area than the wild type (*P*<0.001) and have a circularity index of 0.81 (Table 1), a significant deviation from wild type (*P*<0.001).

Membrane insertion during cellularization still proceeds in *src64* embryos. The depth of membrane invagination and the dynamics of cellularization front ingression is similar to that of wild-type embryos (Fig. 3). These data suggest that *src64*-mediated microfilament contraction does not play a significant role in cellularization front invagination.

tec29 mutants are similar to *src64* mutants, but *src64* is not required to localize Tec29 protein

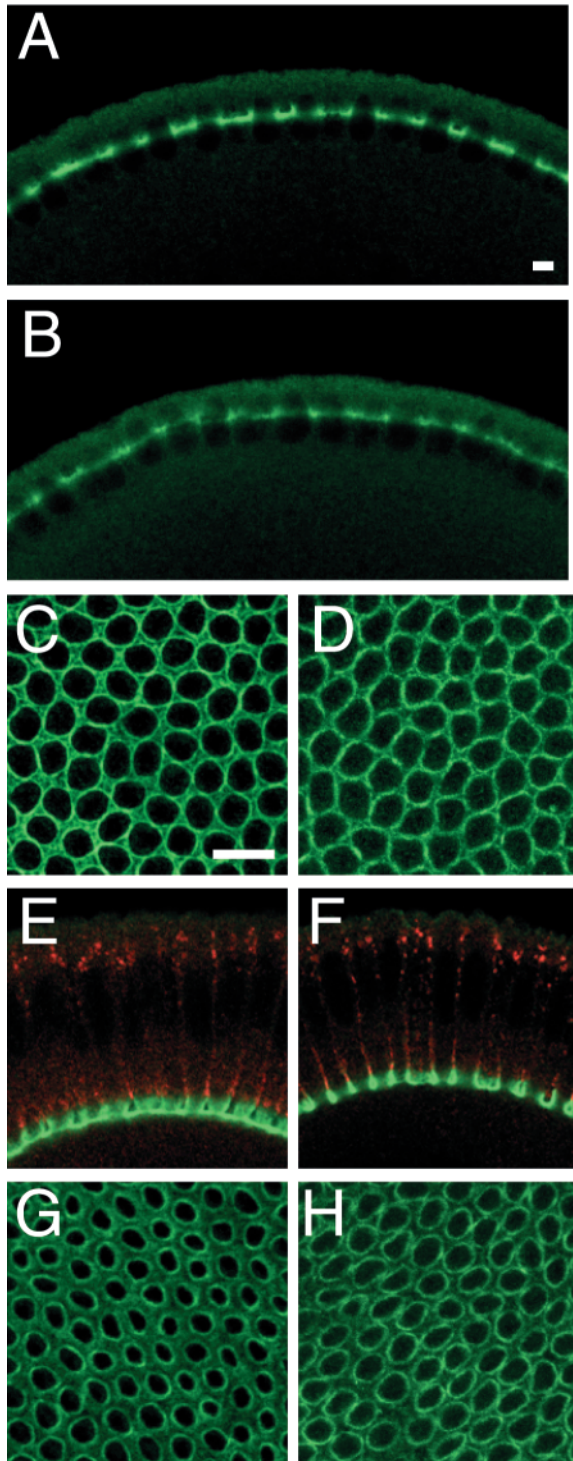*tec29*, a non-receptor tyrosine kinase, is also required for the

Fig. 2. *src64* is required for microfilament ring contraction during cellularization. Cross-sections (A,B,E,F) and projections of confocal sections of the cellularization front (C,D,G,H) of wild-type (A,C,E,G) and *src64^Δ17* mutant (B,D,F,H) embryos, before (A-D) and after (E-H) the cellularization front has passed the bases of the nuclei. Embryos were stained with antibodies to myosin (A-H) and Armadillo (E,F). The early cellularization front, shown by myosin localization, is of uniform depth along the circumference of wild-type embryos (A), but is of non-uniform depth in *src64* mutant embryos (B). The newly formed microfilament rings are round during early cellularization in wild-type embryos (C), but are less rounded in *src64* mutant embryos (D). The late cellularization front is of uniform depth along the circumference of wild-type embryos (E) and the furrow canals are expanded into a flask-like shape, whereas in *src64* mutant embryos, the late cellularization front is also of uniform depth but the furrow canals are unexpanded (F). The microfilament rings of wild-type embryos during late cellularization are round and constricted (G), whereas the microfilament rings of *src64* mutant embryos are less rounded and are not constricted (H), similar to the microfilament rings of *src64* mutant embryos during early cellularization (D). Scale bar: 10 μm.

weakly along the lateral cellular membrane in both wild-type embryos and *src64^Δ17* embryos, suggesting that *src64* does not act to localize Tec29 protein during cellularization (Fig. 1C,D). This is in contrast to the situation in the ovary where Src64 protein acts to localize Tec29 protein to the ring canal (Guarnieri et al., 1998; Roulier et al., 1998). Phosphotyrosine staining is observed at the cellularization front in both wild-type and *src64* mutant embryos (Fig. 1E,F). This suggests that Src64 is not the major source of phosphotyrosine during cellularization as it is in the egg chamber (Dodson et al., 1998; Roulier et al., 1998). Thus both *src64* and *tec29* are required for microfilament ring contraction during cellularization, but *tec29* is localized to the cellularization front independently of *src64* activity.

scraps (anillin) is required for the formation of actin-myosin contractile rings

To determine whether other actin-binding proteins affect microfilament ring contraction in a manner similar to *src64*, we examined the actin-binding protein anillin, which is expressed at the cellularization front in a domain similar that of Src64 (Field and Alberts, 1995; The Flybase Consortium, 2003) (Fig. 1E,F). During later development the anillin protein also localizes to contractile rings during cytokinesis (Field and Alberts, 1995). Anillin is encoded by the gene *scraps*, which is defined by a maternal effect lethal mutation (Schüpbach and Wieschaus, 1989). We analyzed the phenotype of embryos from mothers trans-heterozygous for two strong reduction-of-function mutations of *scraps* (Schüpbach and Wieschaus, 1989). The most informative phenotype of *scraps* mutants is the absence of microfilament rings. This can be readily seen by observing the density and continuity of myosin staining around the basal openings in the cellularization front (compare Fig. 5B with Fig. 2C, and Fig. 5D with Fig. 2G). The furrow canals are collapsed and lack the early bulb-like or the late flask-like morphology of the wild type. Only some furrow canals show strong myosin staining (Fig. 5A,C). Myosin is seen in dense rod-like clumps lying between some of the basal cellular openings (Fig. 5B,D). A similar phenotype has been observed by C. Field (C. Field, personal communication).

morphogenesis of ovarian ring canals and interacts with Src64 protein to control ovarian ring canal growth (Dodson et al., 1998; Guarnieri et al., 1998; Roulier et al., 1998). Cellularizing embryos derived from *tec29^k00206* germline clones have large and non-rounded microfilament rings like those of *src64* embryos (Fig. 4). *tec29* microfilament rings have a circularity index of 0.82 (Table 1), similar to that of *src64* but very different from that of wild-type microfilament rings (*P*<0.001). Tec29 protein is expressed at the cellularization front and more
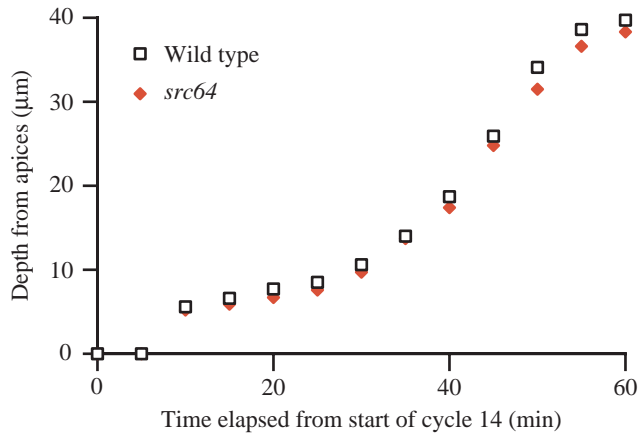
Fig. 3. *src64* is not required for membrane invagination during cellularization. For both wild-type and *src64* embryos, the progress of membrane invagination was measured from the cell apices to the cellularization front and plotted at five minute intervals starting at the beginning of cycle 14 (time=0 minutes) at 25°C. Maximum cellularization depth is obtained just before gastrulation begins in the interval between 55 minutes and 60 minutes. During early cellularization, the s.e.m. values are between 0.1 μm and 0.6 μm, whereas during late cellularization, the s.e.m. values are between 0.5 μm and 1.0 μm.
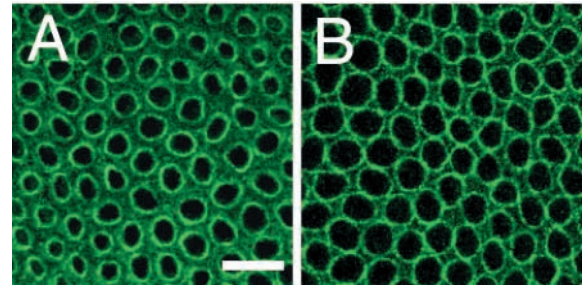

Fig. 4. *tec29* is required for microfilament ring contraction during cellularization. (A,B) Projections of confocal sections of the cellularization front after it has passed the nuclear bases of a wild-type (A) and a *tec29^{k00206}* germline clone (B) embryo. Embryos were stained with antibody to myosin. The microfilament rings of wild-type embryos during late cellularization are round and constricted (A), whereas the microfilament rings of *tec29* germline clone mutant embryos are less rounded and are not constricted (B). Scale bar: 10 μm.

This myosin distribution is similar to that of F-actin in the septin mutant *peanut* during cellularization (Adam et al., 2000), suggesting that both anillin and certain septins play a role in the assembly or maintenance of the microfilament rings.

During early cellularization in *scraps* mutant embryos, the basal cytoplasmic openings are angular and resemble polygons with relatively straight sides (Fig. 5B). Because the sides of these polygons are somewhat uniform in length, they approximate circles and have a circularity index of 0.89 (Table 1), differing only slightly from wild-type microfilament rings. Unlike in *src64* mutants, they are not convoluted or wavy, and indentations are not observed. During late cellularization, the *scraps* phenotype becomes more severe (Fig. 5D) with a circularity index of 0.73 (Table 1), significantly differing from wild type (*P*<0.001). This decrease in circularity reflects an increase in the length of some of the sides of each polygon and a decrease in the length of others so that the basal openings more closely resemble polygons with fewer sides. The sides remain straight and show no waviness that would indicate a lack of tension. Instead, the gradual distortion of the polygons in *scraps* mutants is consistent with stretching due to microfilament contraction in the absence of an organizing structure. The *scraps* phenotype is therefore distinct from that of *src64* mutants, which appear to lack microfilament tension and maintain similar, but deviant, circularities throughout cellularization. This interpretation implies that microfilament rings are not required for microfilament contraction. The low circularity index of later basal openings in *scraps* mutants suggests that microfilament ring structure provides a stabilizing framework for microfilament contraction during the late phase of cellularization.

The premature contraction in *bottleneck* embryos does not require *scraps* (anillin)

We have used mutations in *bottleneck* (*bnk*) to define more

clearly the roles that *src64* and *scraps* play in cellularization. Bnk is a small, highly basic protein that regulates the dynamic restructuring of the actin cytoskeleton so as to control the timing of microfilament ring contraction during late cellularization. It is expressed during early cellularization and its level drops precipitously during the transition to the late phase (Schejter and Wieschaus, 1993b). During early cellularization, Bnk co-localizes with myosin, but extends further apically in the furrow canal (Fig. 6).

The *bnk* phenotype is distinct to that of *src64* or *scraps* in that embryos homozygous for a *bnk* deficiency have a hypercontractile phenotype. The microfilament rings are prematurely constricted during early cellularization (Fig. 7A) (Schejter and Wieschaus, 1993b). The rings squeeze the nuclei into dumbbell shapes during early cellularization, trapping and dragging some of them along with the advancing cellularization front during late cellularization (Fig. 7D) (Schejter and Wieschaus, 1993b). The microfilament rings of early cellularization and late cellularization *bnk* embryos have circularity indices of 0.92 and 0.91 (Table 1), respectively, values that do not differ from those of similarly staged wild-type embryos, even though initially they enclose a much smaller area of open cytoplasm (*P*<0.001).

scraps; bnk double-mutant embryos show a mixture of the phenotypes of both *scraps* and *bnk* embryos (Fig. 7). Like *scraps* embryos, *scraps; bnk* embryos fail to form actin-myosin rings, and instead show dense rod-like aggregates of myosin II lying between some of the non-rounded basal cellular openings. In spite of the absence of contractile rings, *scraps; bnk* embryos still display the premature hypercontraction phenotype characteristic of *bnk* embryos (Fig. 7C). The cytoskeleton surrounding cells in *scraps; bnk* embryos is more contracted, in terms of both area and circularity, than the cytoskeleton surrounding cells in *scraps* embryos. Microfilaments are constricted around dumbbell-shaped nuclei, which are trapped and dragged out of the periphery of the embryo by the cellularization front in *scraps; bnk* double-mutant embryos, as is characteristic of *bnk* embryos (Fig. 7F). The area enclosed by the microfilaments of *scraps; bnk* embryos is significantly less than that of *scraps*
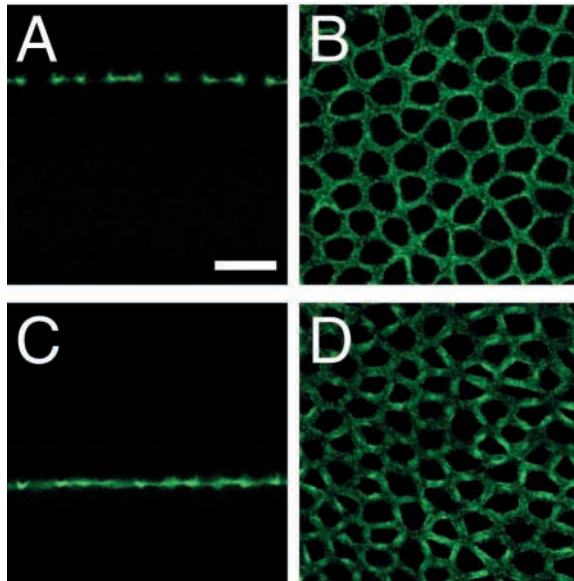
Fig. 5. *scraps* (anillin) is required for the formation of microfilament rings during cellularization. (A-D) Sagittal sections (A,C) and projections of confocal sections of the cellularization front (B,D) of a $scraps^{RS}/scraps^{PQ}$ mutant embryo shortly before (A,B) and after (C,D) the cellularization front has passed the nuclear bases. Embryos were stained with antibody to myosin. (A) The furrow canals of *scraps* mutant embryos during early cellularization are only slightly abnormal. (B) Microfilament rings are not present in *scraps* mutant embryos during early cellularization and the basal lumens are less rounded than in wild-type embryos. Myosin is found in aggregates scattered along the cellularization front (compare with Fig. 2C). (C) The furrow canals of *scraps* mutant embryos during late cellularization are collapsed and lack a flask-like morphology. (D) Microfilament rings are not present in *scraps* mutant embryos during late cellularization; the basal lumens are angular and are less rounded than those during early cellularization in *scraps* mutant embryos (compare with B). Myosin is found in aggregates scattered along the cellularization front (compare with Fig. 2G). Scale bar: 10 µm.

Fig. 6. Bottleneck protein co-localizes to the cellularization front with myosin. Cross-sections (A,C,E) and projections of confocal sections of the cellularization front (B,D,F) before the cellularization front has passed the nuclear bases of wild-type embryos. Embryos were stained with antibodies to Bnk and myosin, and images have been arranged to show Bnk protein (A,B), Myosin (C,D), and merged images of both Bnk and myosin (E,F). (A,B) Bnk is expressed along the entire furrow canal and in microfilament rings during early cellularization. (C,D) Myosin is expressed basal-laterally in the furrow canal and in microfilament rings. (E,F) Bnk and myosin localization overlaps in microfilament rings and overlaps basal-laterally in the furrow canal, but Bnk localization extends farther apically. Scale bar: 10 µm.

embryos ($P<0.001$), but is still larger than that of *bnk* embryos ($P<0.001$). During late cellularization, the circularity index of the basal openings of *scraps; bnk* embryos is 0.90 (Table 1), similar to that of *bnk* embryos, but significantly different from the 0.73 value of *scraps* embryos ($P<0.001$). This difference suggests that the actin-myosin network can still contract in the absence of microfilament rings, but without the efficiency that is conferred by the organization of the cytoskeleton into rings.

The hypercontraction caused by the absence of Bnk protein, coupled with the loss of structural integrity of the cellularization network caused by the absence of anillin and microfilament rings, leads to the apparent tearing of parts of the cellularization network. Several regions of the cytoskeleton are either stretched thin or broken, leaving large gaps in the cellularization front (Fig. 7C). This suggests that the loss of anillin and microfilament rings results in a fragile cytoskeletal structure that unravels in the absence of Bnk. These double-mutant results suggest that Bnk and anillin both play structural roles in the cellularization front, but that neither are necessary for microfilament contraction itself.
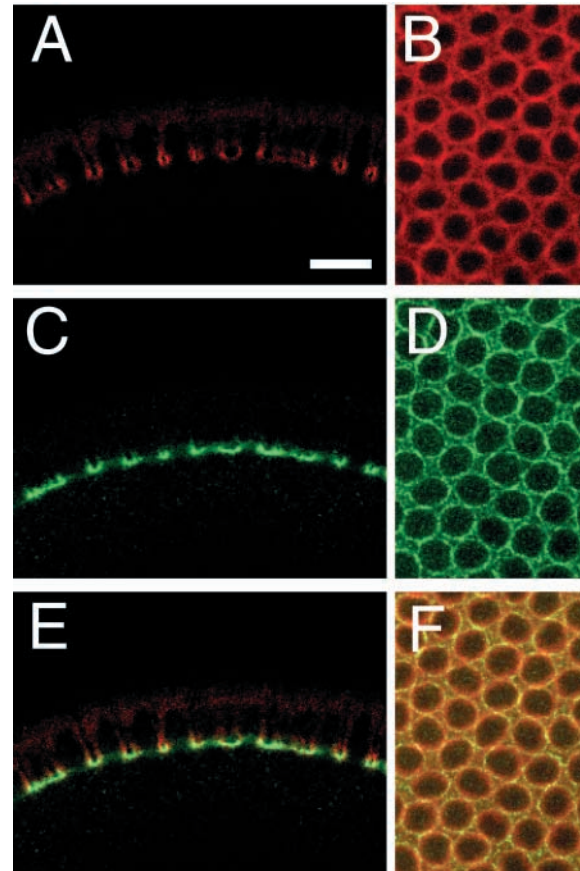
src64 is required for the premature contraction of *bnk* embryos

In restructuring the cytoskeleton during cellularization, Bnk controls the timing of microfilament ring contraction so that basal closure does not occur until after the cellularization front has passed the bases of the nuclei. *bnk* mutants have a prematurely hyperconstricted ring phenotype opposite to the non-constricted ring phenotype of *src64* mutants. *src64 bnk* double-mutant embryos look like *src64* mutant embryos. The *src64 bnk* embryos have the large, non-constricted microfilament rings that appear to be under no tension (Fig. 8). They have a circularity index of 0.85 (Table 1), similar to that of *src64* embryos but different from that of *bnk* embryos ($P<0.001$). A few double-mutant embryos showed some degree of microfilament ring contraction during late cellularization; it is likely that these embryos are the result of some residual
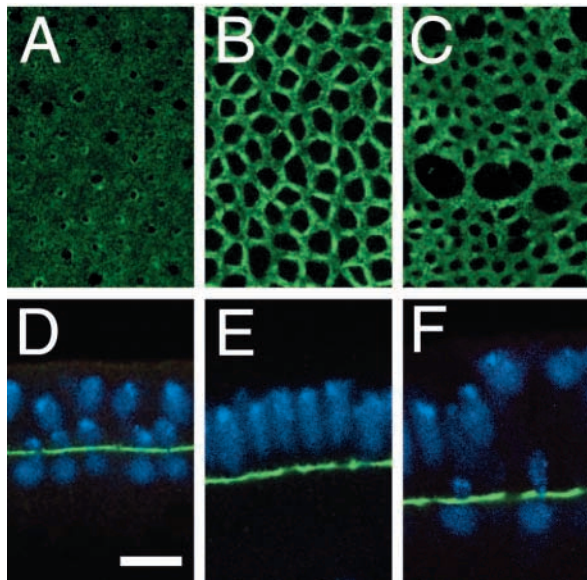
Fig. 7. Phenotypes of *bnk* and *scraps* are co-expressed. Projections of confocal sections of the cellularization front (A-C) and sagittal sections (D-F) of the same *bnk* mutant (A,D), *scraps^{RS}/scraps^{PQ}* mutant (B,E) and *scraps^{RS}/scraps^{PQ}; bnk* double-mutant (C,F) embryos. Embryos were stained with antibody to myosin (A-F) and with Hoechst dye (D-F). (A) Microfilament rings are hypercontracted in *bnk* mutant embryos; some nuclei are constricted into dumbbell shapes by the hyperconstricted microfilament rings and carried out of the periphery by the cellularization front in *bnk* embryos (D). (B) *scraps* mutant embryos showing the absence of microfilament rings, angular basal lumens and a normal nuclear morphology (E). (C) Microfilament rings are not formed in *scraps; bnk* mutant embryos, but the cellularization front still exhibits increased contraction and large gaps in the microfilament network. (F) Despite the absence of microfilament rings in *scraps; bnk* mutant embryos, some nuclei are constricted into dumbbell shapes by the contracted microfilaments and carried out of the periphery. Scale bar: 10 µm.

activity of the reduction-of-function *src64^{Δ17}* allele. The analysis of *src64 bnk* double-mutant embryos demonstrates that the premature hypercontraction of *bnk* requires *src64* activity. The interaction of *bnk* mutation with *src64* and *scraps* reveals the difference between the two genes: *src64* is required for microfilament contraction and *scraps* (anillin) is not. This suggests that *bnk* regulates cytoskeletal contractility during cellularization by counteracting the *src64*-mediated contraction of the microfilament rings.

Discussion

src64 mediates microfilament contraction during cellularization

Our analyses suggest that *src64* and *tec29* are required for tension in the cellularization front during early cellularization, and for the constriction of the basal microfilament rings during late cellularization. Src64 and Tec29, which are present at higher levels in the microfilament rings, might activate actin-myosin contraction or be essential for the ability of the actin-myosin network to contract. Despite a general similarity of form, the cellularization microfilament ring and the oocyte-nurse cell
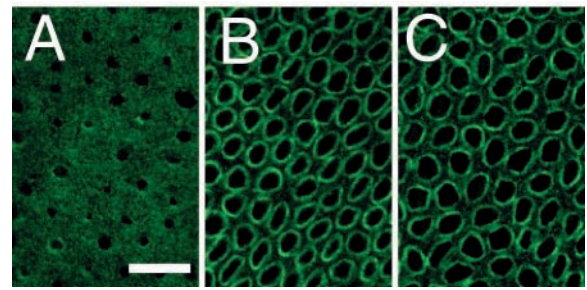

Fig. 8. *src64* activity is required for *bnk* hypercontraction. Projections of confocal sections of the cellularization front (A-C) after it has passed the nuclear bases of a *bnk* mutant (A), a *src64* mutant (B) and a *src64 bnk* double-mutant (C) embryo. Embryos were stained with antibody to myosin (A-C). (A) *bnk* mutant embryo showing hypercontracted microfilament ring phenotype. (B) *src64* mutant embryo showing non-contracted microfilament ring phenotype. (C) *src64 bnk* double-mutant embryo showing a non-contracted microfilament ring phenotype similar to that of *src64* mutant embryos (B). Scale bar: 10 µm.

complex ring canal differ substantially in structure and dynamics. In the ovary, *src64*, and presumably *tec29*, control ring canal expansion by regulating actin polymerization and cross-linking (Kelso et al., 2002; Tilney et al., 1996). It is unlikely that myosin can play a role in this process as myosin-driven sliding of actin filaments would lead to contraction rather than expansion (Tilney et al., 1996). Although myosin is localized to the ring canal, and null mutations in regulatory myosin light chain cause defects in the ring canals, these defects are not severe and do not prevent ring canal assembly or expansion (Hudson and Cooley, 2002; Jordan and Karess, 1997; Edwards and Kiehart, 1996). Thus, despite a similar involvement of *src64* and *tec29*, it is unlikely that microfilament ring constriction and ring canal expansion are mechanistically similar.

scraps (anillin) is required for the formation of stable contractile microfilament rings

Anillin, which localizes to the cellularization front and shows higher concentration in the contractile microfilament rings, is required for proper cellularization. Anillin bundles actin filaments and may stabilize these filaments during actin-myosin contraction (Field and Alberts, 1995). On the basis of these observations, we conclude that in the absence of anillin, stable contractile microfilament rings do not form; instead the contractile protein myosin is irregularly distributed in aggregates throughout the cellularization front. Strikingly, loss of anillin in *bnk* embryos does not suppress the severe early contraction defect seen in *bnk* embryos. In the absence of the structure provided by these rings, the contraction of the microfilaments is uneven, leading to increasing defects in the shape of the basal openings as cellularization progresses. This suggests that anillin is not required for the ability of the microfilaments of the cellularization network to contract, only for their organization into stable rings.

src64 and *bnk* oppose each other during early cellularization

The phenotypes presented in this paper support a model in which *src64* and *bnk* oppose each other to control contraction of the early cellularization network. Double-mutant analysis reveals that
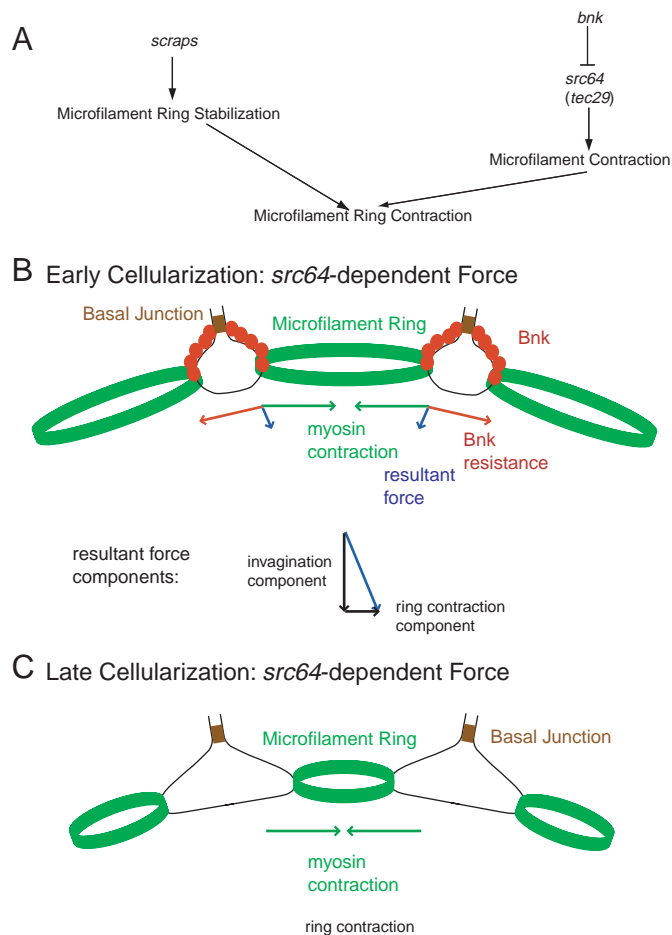
A

scraps

bnk

↓

src64
(tec29)

Microfilament Ring Stabilization

↓

Microfilament Contraction

↓

Microfilament Ring Contraction

B Early Cellularization: src64-dependent Force

Basal Junction   Microfilament Ring   Bnk

myosin contraction   Bnk resistance

resultant force

resultant force components: invagination component   ring contraction component

C Late Cellularization: src64-dependent Force

Microfilament Ring   Basal Junction

myosin contraction

ring contraction

Fig. 9. Model for *src64*-dependent and *src64*-independent forces acting during cellularization. (A) Epistasis pathway for microfilament contraction during cellularization. *src64* is epistatic to *bnk* in the pathway controlling microfilament ring contraction. *tec29* is speculatively placed in the pathway with *src64* as Tec kinases are generally activated by Src kinases, although this has not been experimentally confirmed for *Drosophila* cellularization. *scraps* (anillin) has been placed in a parallel pathway to *bnk* and *src64* because it plays an important, but indirect, role in microfilament ring contraction by stabilizing microfilament rings. In the absence of anillin, microfilament rings are not formed, but the disorganized microfilaments still have the ability to contract in the absence of *bnk* activity. *peanut* (*pnut*) also acts in this process. (B) Mechanical model for the interaction of Bnk and Src64 protein during early cellularization. See Discussion for details. (C) Mechanical model for the interaction of Bnk and Src64 protein during late cellularization. See Discussion for details.

src64 is epistatic to *bnk* (Fig. 9A). Bnk acts only to restrain and partially redirect Src64-mediated ring constriction. The fact that cellularization proceeds in *src64* and *tec29* mutants suggests that a force other than microfilament ring contraction is sufficient to drive cellularization front invagination. This force may be a result of the insertion of membrane (Lecuit and Wieschaus, 2000; Sisson et al., 2000), or may be due to the action of plus-end directed microtubular motors (Mazumdar and Mazumdar, 2002; Foe et al., 2000; Foe et al., 1993), or some combination of both.

Most models for cellularization invoke a role for myosin contraction during the ring constriction and basal closure that

occur during late stages of the process; a role during early stages is more controversial. The early phenotype of *src64* mutants, if our interpretation is correct, suggests a role for microfilament ring contraction in the early stages as well, acting both to coordinate the invagination of the furrow canals by maintaining tension along the cellularization front and to direct their invagination inward. This force is a product of the interaction of *src64*-dependent, myosin-mediated contraction of the microfilament rings and resistance to this contraction exerted by Bnk protein, which acts as a linker between the rings. These forces oppose each other at all points along the contractile microfilament ring network, generating a dynamic tension over the entire network, keeping it taut and driving the minimization of its surface area. The addition of these force vectors acting on a cross-section of one ring on a curved surface produces a resultant vector directed both toward the interior of the embryo (the center of the circular cross-section) and toward the center of the microfilament ring. The first component of the resultant force vector is the *src64*-mediated force that provides direction to the invagination that follows the increase in surface area produced by membrane insertion during early cellularization (Fig. 9B). The other component of the resultant force vector is in the plane of the microfilament ring, coordinating constriction about the entire circumference of the embryo and driving a small degree of constriction consistent with the decrease in cellularization front surface area during invagination (Fig. 9B).

As the cellularization front passes the bases of the nuclei and cellularization shifts into its late phase of rapid progression (Lecuit and Wieschaus, 2000), Bnk expression is shut off and the protein is rapidly degraded and removed from the cellularization network (Schejter and Wieschaus, 1993b). In the absence of Bnk protein, there is no force resisting microfilament ring contraction, so it no longer contributes to driving cellularization front invagination. The *src64*-mediated force is now directed along the radii of the rings, leading to their constriction. This constriction pulls the membrane toward the center of the base of the cell, expanding the furrow canals and leading to basal closure (Fig. 9C). The *src64*-independent force (membrane addition or microtubular motors) may be the only force now driving the inward invagination of the cellularization front.

In conclusion, our data define the differing roles that *src64*, *tec29* and anillin play in the cytoskeletal dynamics of *Drosophila* cellularization, and reveal more precisely the role that the cytoskeleton plays in the formation of the cellular blastoderm. These data establish that microfilament ring organization and contraction are crucial to basal closure of the blastoderm cells during cellularization. However, these data also suggest that membrane invagination can proceed, though abnormally and less efficiently, in the absence of microfilament organization or contraction. It will be interesting to determine what the comparative roles and contributions of membrane insertion and microtubular motors are to the progression of the cellularization front.

References

Adam, J. C., Pringle, J. R. and Peifer, M. (2000). Evidence for fundamental differentiation among *Drosophila* septins in cytokinesis and cellularization. *Mol. Biol. Cell* **11**, 3123-3135.

Baba, K., Takeshita, A., Majima, K., Ueda, R., Kondo, S., Juni, N. and Yamamoto, D. (1999). The *Drosophila* Bruton's tyrosine kinase (Btk) homolog is required for adult survival and male genital formation. *Mol. Cell. Biol.* **19**, 4405-4413.

Dodson, G. S., Guarnieri, D. J. and Simon, M. A. (1998). *Src64* is required for ovarian ring canal morphogenesis during *Drosophila* oogenesis. *Development* **125**, 2883-2892.

Edwards, K. A. and Kiehart, D. P. (1996). *Drosophila* nonmuscle myosin II has multiple essential roles in imaginal disc and egg chamber morphogenesis. *Development* **122**, 1499-1511.

Field, C. M. and Alberts, B. M. (1995). Anillin, a contractile ring protein that cycles from the nucleus to the cell cortex. *J. Cell Biol.* **131**, 165-178.

The Flybase Consortium (2003). The flybase database of the *Drosophila* genome projects and community literature. *Nucl. Acids Res.* **31**, 172-175.

Foe, V. E., Odell, G. M. and Edgar, B. A. (1993). Mitosis and morphogenesis in the *Drosophila* embryo: point and counterpoint. In *The Development of* Drosophila melanogaster (ed. M. Bate and A. Martinez Arias), pp. 149-300. Cold Spring Harbor, NY: Cold Spring Harbor Laboratory Press.

Foe, V. E., Field, C. M. and Odell, G. M. (2000). Microtubules and mitotic cycle phase modulate spatiotemporal distributions of F-actin and myosin II in *Drosophila* syncytial blastoderm embryos. *Development* **127**, 1767-1787.

Frame, M. C. (2002). Src in cancer: deregulation and consequences for cell behavior. *Biochim. Biophys. Acta* **1602**, 114-130.

Frame, M. C., Fincham, V. J., Carragher, N. O. and Wyke, J. A. (2002). v-*src*'s hold over actin and cell adhesion. *Nat. Rev. Mol. Cell Biol.* **3**, 233-245.

Fullilove, S. L. and Jacobson. A. G. (1971). Nuclear elongation and cytokinesis in *Drosophila montana*. *Dev. Biol.* **26**, 560-570.

Gregory, R. J., Kammermeyer, K. L., Vincent, W. S., III and Wadsworth, S. G. (1987). Primary sequence and developmental expression of a novel *Drosophila melanogaster src* gene. *Mol. Cell. Biol.* **7**, 2119-2127.

Guarnieri, D. J., Dodson, G. S. and Simon, M. A. (1998). *Src64* regulates the localization of a Tec-family kinase required for *Drosophila* ring canal growth. *Mol. Cell* **1**, 831-840.

Harrison, S. C. (2003). Variation on a Src-like theme. *Cell* **112**, 727-740.

Hudson, A. M. and Cooley, L. (2002). Understanding the function of actin-binding proteins through genetic analysis of *Drosophila* oogenesis. *Annu. Rev. Genet.* **36**, 455-488.

Jordan, P. and Karess, R. (1997). Myosin light chain-activating phosphorylation sites are required for oogenesis in *Drosophila*. *J. Cell Biol.* **139**, 1805-1819.

Katzen, A. L., Kornberg, T. and Bishop, J. M. (1990). Diverse expression of *dsrc29A*, a gene related to *src*, during the life cycle of *Drosophila melanogaster*. *Development* **110**, 1169-1183.

Kelso, R. J., Hudson, A. M. and Cooley, L. (2002). *Drosophila* Kelch regulates actin organization via Src64-dependent tyrosine phosphorylation. *J. Cell Biol.* **156**, 703-713.

Lecuit, T. and Wieschaus, E. (2000). Polarized insertion of new membrane from a cytoplasmic reservoir during cleavage of the *Drosophila* embryo. *J. Cell Biol.* **150**, 849-860.

Lindsley, D. L. and Zimm, G. A. (1992). *The genome of* Drosophila melanogaster. San Diego: Academic Press.

Mahajan-Miklos, S. and Cooley, L. (1994). Intercellular cytoplasm transport during *Drosophila* oogenesis. *Dev. Biol.* **165**, 336-351.

Mazumdar, A. and Mazumdar, M. (2002). How one becomes many: blastoderm cellularization in *Drosophila melanogaster*. *BioEssays* **24**, 1012-1022.

Nose, A., Takeichi, M. and Goodman, C. S. (1994). Ectopic expression of Connectin reveals a repulsive function during growth cone guidance and synapse formation. *Neuron* **13**, 525-539.

Oda, H., Uemura, T., Harada, Y., Iwai, Y. and Takeichi, M. (1994). A *Drosophila* homolog of cadherin associated with armadillo and essential for embryonic cell-cell adhesion. *Dev. Biol.* **165**, 716-726.

Robinson, D. N., Cant, K. and Cooley, L. (1994). Morphogenesis of *Drosophila* ovarian ring canals. *Development* **120**, 2015-2025.

Robinson, D. N. and Cooley, L. (1996). Stable intercellular bridges in development: the cytoskeleton lining the tunnel. *Trends Cell Biol.* **6**, 474-479.

Rothwell, W. F., Fogarty, P., Field, C. M. and Sullivan, W. (1998). Nuclear fallout, a *Drosophila* protein that cycles from the cytoplasm to the centrosomes, regulates cortical microfilament organization. *Development* **125**, 1295-1303.

Roulier, E. M., Panzer, S. and Beckendorf, S. K. (1998). The Tec29 tyrosine kinase is required during *Drosophila* embryogenesis and interacts with Src64 in ring canal development. *Mol. Cell* **1**, 819-829.

Schejter, E. D. and Wieschaus, E. (1993a). Functional elements of the cytoskeleton in the early *Drosophila* embryo. *Annu. Rev. Cell Biol.* **9**, 67-99.

Schejter, E. D. and Wieschaus, E. (1993b). *bottleneck* acts as a regulator of the microfilament network governing cellularization of the *Drosophila* embryo. *Cell* **75**, 373-385.

Schüpbach, T. and Wieschaus, E. (1989). Female sterile mutations on the second chromosome of *Drosophila melanogaster*. I. Maternal effect mutations. *Genetics* **121**, 101-117.

Simon, M. A., Kornberg, T. and Bishop, J. M. (1983). Three loci related to the *src* oncogene and tyrosine-specific protein kinase activity in *Drosophila*. *Nature* **302**, 837-839.

Simon, M. A., Drees, B., Kornberg, T. and Bishop, J. M. (1985). The nucleotide sequence and the tissue-specific expression of *Drosophila* c-*src*. *Cell* **42**, 831-840.

Sinka, R., Jankovics, F., Somogyi, K., Szlanka, T., Lukácsovich, T. and Erdélyi, M. (2002). *poirot*, a new regulatory gene of *Drosophila oskar* acts at the level of the short Oskar protein isoform. *Development* **129**, 3469-3478.

Sisson, J. C., Field, C., Ventura, R., Royou, A. and Sullivan, W. (2000). Lava Lamp, a novel peripheral golgi protein, is required for *Drosophila melanogaster* cellularization. *J. Cell Biol.* **151**, 905-917.

Smith, C. I. E., Islam, T. C., Mattsson, P. T., Mohamed, A. J., Nore, B. F. and Vihinen, M. (2001). The Tec family of cytoplasmic tyrosine kinases: mammalian Btk, Bmx, Itk, Tec, Txk and homologs in other species. *BioEssays* **23**, 436-446.

Sokol, N. S. and Cooley, L. (1999). *Drosophila* Filamin encoded by the *cheerio* locus is a component of ovarian ring canal. *Curr. Biol.* **9**, 1221-1230.

Takahashi, F., Endo, S., Kojima, T. and Saigo, K. (1996). Regulation of cell-cell contacts in developing *Drosophila* eyes by *Dsrc41*, a new, close relative of vertebrate c-*src*. *Genes Dev.* **10**, 1645-1656.

Tateno, M., Nishida, Y. and Adachi-Yamada, T. (2000). Regulation of JNK by Src during *Drosophila* development. *Science* **287**, 324-327.

Thomas, S. M., Soriano, P. and Imamoto, A. (1995). Specific and redundant roles of Src and Fyn in organizing the cytoskeleton. *Nature* **376**, 267-271.

Thomas, S. M. and Brugge, J. S. (1997). Cellular functions regulated by Src family kinases. *Annu. Rev. Cell Dev. Biol.* **13**, 513-609.

Tilney, L. G., Tilney, M. S. and Guild, G. M. (1996). Formation of actin filament bundles in the ring canals of developing *Drosophila* follicles. *J. Cell Biol.* **133**, 61-74.

Vincent, W. S., III, Gregory, R. J. and Wadsworth, S. C. (1989). Embryonic expression of a *Drosophila src* gene: alternate forms of the protein are expressed in segmented stripes and in the nervous system. *Genes Dev.* **3**, 334-347.

Wadsworth, S. C., Madhavan, K. and Bilodeau-Wentworth, D. (1985). Maternal inheritance of transcripts from three *Drosophila src*-related genes. *Nucl. Acids Res.* **13**, 2153-2170.

Warn, R. M. and Robert-Nicoud, M. (1990). F-actin organization during the cellularization of the *Drosophila* embryo as revealed with a confocal laser scanning microscope. *J. Cell Sci.* **96**, 35-42.

Wieschaus, E. and Nusslein-Volhard, C. (1998). Looking at embryos. In Drosophila*: A Practical Approach*, 2nd edn (ed. D. B. Roberts), pp. 179-214. Oxford: Oxford University Press.

Young, P. E., Pesacreta, T. C. and Kiehart, D. P. (1991). Dynamic changes in the distribution of cytoplasmic myosin during *Drosophila* embryogenesis. *Development* **111**, 1-14.

Zallen, J. A., Cohen, Y., Hudson, A. M., Cooley, L., Wieshaus, E. and Schejter, E. D. (2002). SCAR is a primary regulator of Arp2/3-dependent morphological events in *Drosophila*. *J. Cell Biol.* **156**, 689-701.